

Altered expression of two zinc transporters, SLC30A5 and SLC30A6, underlies a mammary gland disorder of reduced zinc secretion into milk

Loveleen Kumar¹ · Agnes Michalczyk¹ · Jill McKay² · Dianne Ford³ · Taiho Kambe⁴ · Lee Hudek¹ · George Varigos⁵ · Philip E. Taylor¹ · M. Leigh Ackland¹

Received: 15 May 2015 / Accepted: 14 August 2015 / Published online: 29 August 2015
© Springer-Verlag Berlin Heidelberg 2015

Abstract Two cases of zinc deficiency in breastfed neonates were investigated where zinc levels in the mothers' milk were reduced by more than 75 % compared to normal. The objective of this study was to find the molecular basis of the maternal zinc deficiency condition. Significant reductions in mRNA expression and protein levels of the zinc transporters SLC30A5 and SLC30A6 were found in maternal tissue, suggesting a causal link to the zinc-deficient milk. Novel splice variants of the SLC30A6 transcript were detected. No modifications were found in coding regions, or in transcription binding sites of promoter regions or in 5' and 3' untranslated regions of both transporters in lymphoblasts and fibroblasts isolated from both mothers. Altered DNA methylation in SLC30A5 at two CpG sites was detected and may account for the reduced levels of SLC30A5 mRNA and protein in lymphoblasts. Reduced SLC30A6 mRNA and protein levels in lymphoblasts may be secondary to reduced SLC30A5 expression, as they function as a heterodimer in zinc transport. In conclusion, two cases of zinc deficiency are

linked to low levels of the SLC30A5 and SLC30A6 zinc transporters. These two zinc transporters have not been previously associated with zinc deficiency in milk.

Keywords Zinc · Zinc transporters · Mammary · Neonatal zinc deficiency · DNA methylation · Lactation

Abbreviations

TNAP	Tissue non-specific alkaline phosphatase activity
SLC	Solute carrier
UTR	Untranslated region
MRE	Metal-responsive element
PRE	Progesterone-responsive element
GRE	Gonadotrophin-responsive element
IRE	Insulin-responsive element

Introduction

The most frequently occurring form of zinc deficiency is caused by nutritional insufficiency. In some cases however, zinc deficiency is found in breastfed babies, who present with symptoms characteristic of nutritional zinc deficiency, including dermatitis, diarrhoea, alopecia, loss of appetite, impaired immune function and neuropsychiatric changes (Aggett et al. 1980; Prasad 1985). This form of zinc deficiency is a consequence of reduced levels of zinc in the maternal milk and has been reported in preterm babies (27- to 33-week gestation) (Aggett et al. 1980; Connors et al. 1983; Heinen et al. 1995; Parker et al. 1982; Weymouth et al. 1982; Zimmerman et al. 1982) and less commonly in full-term babies (Bye et al. 1985; Glover and Atherton 1988; Khoshoo et al. 1992; Stevens and Lubitz 1998).

✉ M. Leigh Ackland
leigha@deakin.edu.au

¹ Centre for Cellular and Molecular Biology, School of Life and Environmental Sciences, Deakin University, 221 Burwood Highway, Burwood, VIC 3125, Australia

² Institute of Health and Society, Newcastle University, Newcastle upon Tyne, UK

³ Institute for Cell and Molecular Biosciences, Newcastle University, Newcastle upon Tyne, UK

⁴ Graduate School of Biostudies, Kyoto University, Kyoto 606-8502, Japan

⁵ Department of Dermatology, Royal Melbourne Hospital, Grattan Street, Parkville, Melbourne, VIC 3050, Australia

Pedigree analysis indicates that the condition is inherited (Sharma et al. 1988). Zinc levels in the maternal milk of zinc-deficient breastfed babies were <40 % that of normal milk at matched weeks of lactation (Weymouth et al. 1982; Zimmerman et al. 1982). Maternal zinc deficiency was not responsible for the low zinc levels in breast milk (Weymouth et al. 1982; Zimmerman et al. 1982).

Zinc deficiency caused by reduced zinc levels in the milk is associated with defects in *SLC30A2* (ZnT2). A missense mutation that substituted a conserved histidine, at amino acid 54, with arginine (H54R) was reported (Chowanadisai et al. 2006). The production of zinc-deficient milk was also linked to a glycine to arginine substitution (G87R) (Lasry et al. 2012). Two novel missense mutations in the *SLC30A2* (ZnT2) genes were reported in a Japanese mother with milk zinc levels reduced below 90 % of normal (Isumura et al. 2013).

An inherited disorder of mice with similar phenotype to the human condition of reduced secretion of zinc into milk has been described (Piletz and Ganschow 1978). Newborn pups that were nursed on 'lethal milk', homozygous mutant dams (lm/lm), developed dermatitis, alopecia and showed stunted growth, leading to death within a week and a defect in the secretion of zinc from the mammary gland, were demonstrated (Ackland and Mercer 1992; Lee et al. 1992). A nonsense mutation at arginine codon 297 in the *Slc30a4* (ZnT4) zinc transporter, causing premature protein termination, was associated with the mouse disorder (Huang and Gitschier 1997).

A study of the human orthologue (*SLC30A4*) of the murine *Slc30a4* gene in two mothers with zinc-deficient milk, including sequence analysis of cDNA, real-time PCR and Western blot analysis, showed no differences between patient and normal control cells, which concluded that unlike the mouse disorder, defects in *SLC30A4* were not responsible for the human disorder of reduced secretion of

zinc into milk (Michalczyk et al. 2003). In these patients, it is likely, therefore, that the maternal mammary gland defect in zinc secretion is different from the 'lethal milk' mouse model and that other candidate *SLC30A* transporters may underlie the mammary zinc transport defect. In our study, we sequenced *SLC30A2* to detect mutations associated with these two unrelated mothers and investigated whether modifications to other *SLC30A* zinc exporters underlie this mammary gland disorder.

Materials and methods

Case histories

The following clinical presentation of two cases of zinc deficiency has previously been reported (Michalczyk et al. 2003). Infant 1 was born premature at 36 weeks and was breastfed for three months. A red, necrolytic rash developed at 2 months of age (Fig. 1a, b). Zinc deficiency was confirmed at 3 months post-partum by tests showing zinc blood levels of 4.5 $\mu\text{mol/l}$ (0.29 $\mu\text{g/ml}$) (reference range 10.3–18.1 $\mu\text{mol/l}$; 0.67–1.18 $\mu\text{g/ml}$). The level of breast milk zinc from the mother of Infant 1 (Mother 1) was 0.29 $\mu\text{g/ml}$, which was less than one-quarter that of the normal zinc level (1.35 $\mu\text{g/ml}$) at the corresponding stage of lactation. Treatment of the infant with zinc (50 mg/day) resulted in a dramatic improvement in the rash within 3 days. Infant 2 was born premature at 37-week gestation and developed dermatitis affecting the face and perioral skin, with scalp scale and similar symptoms as that of Infant 1. The maternal milk zinc level (Mother 2) at 7 months was 0.2 $\mu\text{g/ml}$, which was considerably less than the normal zinc level (0.85 $\mu\text{g/ml}$). On commencing treatment with zinc (50 mg/day), the rash cleared in 3 days



Fig. 1 Zinc-deficient Infant 1 born at 37 weeks gestation, showing necrolytic rash at extremities with blistering and desquamation (a) and (b)

and hair started to grow fully. It is interesting to note that both mothers who produced zinc-deficient milk had no clinical symptoms of zinc deficiency themselves.

Sample collection and cell culture

Ethical approval for the collection of blood and skin biopsies was obtained from Deakin University, Melbourne, Australia (EC32-2000), and the Royal Children's Hospital, Parkville, Australia (ERC 2025B). Fibroblast and lymphoblast cell lines from patients (Mother 1 and Mother 2) and respective healthy controls (three lymphoblast and three fibroblast lines) were established as previously described (Michalczyk et al. 2003). The human epithelial breast cell line PMC42-LA, a variant of PMC42 cell line, originally derived from a pleural effusion (Whitehead et al. 1983). Normal resting breast tissue (BT) was obtained from breast biopsies performed for diagnosis of breast disease.

Tissue non-specific alkaline phosphatase assay (TNAP)

Fibroblast and lymphoblast from patients and pooled controls, PMC42-LA and BT, were collected for tissue non-specific alkaline phosphatase (TNAP) activity. Collected pellets were lysed using ALP lysis buffer (10 mM Tris-HCl, pH 7.5, 0.5 mM MgCl₂, 0.1 % Triton-X 100). Twenty micrograms of total cellular proteins was pre-incubated in lysis buffer for 10 min at room temperature. A 100 µl volume of substrate solution (2 mg/ml *p*-nitrophenyl phosphate in 1 M diethanolamine buffer, pH 9.8, containing 0.5 mM MgCl₂) (Sigma-Aldrich; Sydney, Australia) was added. After 10-min incubation at room temperature, *p*-nitrophenol, released by TNAP, was measured at 405 nm absorbance. Shrimp ALP (Roche Applied Sciences, Germany) was used as a standard.

DNA and total RNA isolation

DNA was isolated from patient and pooled control fibroblast and lymphoblast cells using the Wizard[®] Genomic DNA Purification Kit (Promega) following the manufacturer's instructions. DNA concentrations were checked on a nanospec (Nanodrop 1000, Thermo Scientific) at wavelengths of 260/280 nm.

Total RNA was extracted from patient and pooled control fibroblast and lymphoblast cells using a Qiagen RNeasy Mini kit (Qiagen), following the manufacturer's instructions. Extracted RNA was purified using RNeasy kit. The purified RNA concentrations were estimated on a Nanospec (Nanodrop 1000, Thermo Scientific) at wavelengths of 260/280 nm.

Reverse transcription

Two micrograms of purified RNA from patient and control samples was reverse-transcribed using a High-Capacity cDNA reverse transcription kit (Applied Biosystems) per 20 µl reaction according to manufacturer's protocol. The reaction was carried out at 25 °C for 10 min, 37 °C for 120 min, 85 °C for 5 min.

Real-time PCR

Amplification reactions were performed with 1 × SYBR Green PCR Master Mix (Applied Biosystem, Warrington, UK), 3 µm of forward and reverse primers sequences (see Table 1) and 20 ng cDNA (RNA content prior to RT step). Samples were analysed in triplicate using GeneAmp 5700 Sequence Detection System (Applied Biosystems). An internal control of β-actin (see Table 1 for primer sequences) was used to normalize mRNA quantities and efficiency of reverse transcription. Amplification was performed for the ten known human zinc exporters (SLC30A1 to SLC30A10) from lymphoblasts and fibroblasts of patients and the control. Fluorescence produced by incorporation of SYBR green dye into double-stranded DNA was recorded after the elongation phase of each repetitive cycle. The specificity of each reaction was determined by analysis of the melting point dissociation curve generated at the end of each PCR. The threshold cycle value (C_T), defined as the cycle number when fluorescence levels exceed the threshold value, was calculated after each reaction. The C_T value of β-actin was subtracted from the transporter C_T value to produce ΔC_T for each sample. The relative mRNA expression level of each sample was calculated using the equation $2^{-\Delta\Delta C_T}$, where $\Delta\Delta C_T$ is the difference between the control ΔC_T and the patient's ΔC_T . A *t* test was applied for statistical analysis of the results.

PCR and sequencing for coding and promoter regions

The coding regions of SLC30A2, SLC30A5 and SLC30A6, and promoter regions of SLC30A5 and SLC30A6 genes (4000 bp upstream) were amplified. PCR amplification was performed using 55 pmol of forward and reverse primers (Table 1). They were then added to the PCR mixture consisting of 200 ng of DNA, 200 µm of each dNTP, PCR buffer, 1.5 mM MgCl₂ and 1 U Taq DNA polymerase (Sigma-Aldrich, Melbourne, Australia). The following PCR amplification conditions were applied: one cycle at 94 °C for 3 min, 35 cycles at 94 °C for 45 s, annealing temperature for 30 s, 72 °C for 60 s, with final extension at 72 °C for 10 min. PCR products were run on 1 % agarose

Table 1 Primers used for RT-PCR and real-time PCR

Forward primer	Reverse primer	PCR product length (bp)
ZnT1-RealF1 CTGGTGAACGCCATCTTCCT	ZnT1-RealR1 CAATCTCGTGCGGCTCGAT	183
ZnT2-RealF2 TGTGATCCTGGTGTGATGGA	ZnT2-RealR2 CAGGCTGTGCAGGGCTTCT	103
ZnT3-RealF1 CACCTCCGAGACGTTCTTC	ZnT3-RealR1 GGCACCGACAACAGCGTAT	90
ZnT4-RealF2 AACCAGTCTGGTCACCGTCA	ZnT4-RealR2 CTATCCTGCCCATGGTTACG	93
ZnT5-RealF1 CCAGCGCTCGATTAACAAAATA	ZnT5-RealR1 TGTGAACAGCTTTTAGGAGATCA	134
ZnT6-RealF2 TCCTTTTTTGCAAGTTGTTACG	ZnT6-RealR2 AAGCAGGAAGCCAGTACATATCAAG	111
ZnT7-RealF1 TTGCCCTGTCCATCAAAG	ZnT7-RealF2 AGACCTAAACCAGCCCGAGATC	81
ZnT8-RealF1 ACCATGGTCATAGCTTACGA	ZnT8-RealF2 CGAATCAGTACCGCAATTTA	157
ZnT9-RealF1 AACGGCATTAGCATCGTATG	ZnT9-RealF2 GTAACGTGAAACTTGGATCGAT	114
ZnT10-RealF1 AGCTTTGCAATGGCTTAGG	ZnT10-RealF2 GTACCCTAACTGGTTAATATCG	95
βAC-RealF GACAGGATGCAGAACGAGAT	βAC-RealR TGATCCACATCTGCTGGAAGGT	138
GAPDH-RealF CCACCCATGGCAAATTCC	GAPDH-RealR TGGGATTTCCATTGATGACAA	145
ZnT5-A GCAGCGGCGAGACATGAGGAG	ZnT5-B CACTACCACTCCTCCAGACAG	1113
ZnT5-C TCTCTCATTATGCCTTTTGC	ZnT5-D GCATCTTTAATCAGTGAACA	1125
ZnT5-E CAGCATTGGTGTGATCGTATC	ZnT5-F AAGATTCCTTGATCCAGTAGT	629
ZnT6-A AGAACGGCTTCCGGCGGG	ZnT6-B GAGGCATTGGGATTACGTGA	1131
ZnT6-C AAGTCTTACTCCAGACAACA	ZnT6-D AATGTGAACAAGACTACTAT	758
ZnT2-1F CGTCCTCACTCAGCAACACC	ZnT2-1R TCTTCGTTCCCTCACCTCAC	658
ZnT2-2F AGGACTCCCATTCCCCTATC	ZnT2-2R AGGGAGAATAACGTCACCCATGT	582
ZnT2-3F ATATTGGTGGCCCATTTTAC	ZnT2-3R ACAGAGGCCATGGTTGACAT	503
ZnT2-4F ATATGAGGGGTGGGGTAAGG	ZnT2-4R ACAGCTCCCAGTGTCTTGG	527
ZnT2-5F GCCCTATCTCTCATGGCTGT	ZnT2-5R CCACCTACCCTTCAGGTTGT	533
ZnT2-6F TTCTGAACTGTGGTCTGTCCCT	ZnT2-6R GAACTGCCAGACCTGAAAGC	501
ZnT2-7F TCAGTGTTAAGAGTGGAGAGGAA	ZnT2-7R AACCCAGCCTCAGTTTCTT	530

Table 1 continued

Forward primer	Reverse primer	PCR product length (bp)
<i>ZnT2-8F</i> TACCTGGCCAGAGGAATGGAA	<i>ZnT2-8R</i> GAAAGGGAACATTTGGCTCA	848
<i>ZnT2-9F</i> TATGAATCTGAGCCCCTCCA	<i>ZnT2-9R</i> CAAGTGACCAAACCCACCTC	912
<i>ZnT2-C5F</i> ACTGGTGTACCTGGCTGTGG	<i>ZnT2-C5R</i> CCGAGTAGTCTCGATCTGG	210
<i>ZnT5-P1F</i> TCAGGCTCCTCTCATTCTCC	<i>ZnT5-P1R</i> TGTTTCTTACAGCCCCGAAC	1256
<i>ZnT5-P2F</i> GGCAAGTCCATAAAGTGAAGC	<i>ZnT5-P2R</i> CTGAGGAGGAGAATGGCTTG	1189
<i>ZnT5-P3F</i> CAAGCCATTCTCCTCCTCAG	<i>ZnT5-P3R</i> GACCAAAATTTGCCTCCTCA	1098
<i>ZnT5-P4F</i> GAGACAGGGTTTGCCATGT	<i>ZnT5-P4R</i> CAAGCAGAACTCGCCTTT	1045
<i>ZnT5-P5F</i> TGGGAATACAGCCCAGTAGG	<i>ZnT5-P5R</i> GACCAGATTAATGCCAGAGC	645
<i>ZnT5-P6F</i> CCATACTGCCAGACCCTTA	<i>ZnT5-P6R</i> ATGGCGAAACCCTGTCTCTA	432
<i>ZnT5-P7F</i> AGCCACAAAAGCAGTCACCT	<i>ZnT5-P7R</i> AAAATTTGCCTCCTCAGCAA	684
<i>ZnT5-P8F</i> AGGAGAATCGCTTGAACCTG	<i>ZnT5-P8R</i> GGAGAAAAGTGCATCCTGAGC	750
<i>ZnT5-P9F</i> TCCCAAATTTCCCAGAGTA	<i>ZnT5-P9R</i> GTGGGGAGCTTACAAAATGG	243
<i>ZnT5-P10F</i> CCATACTGCCAGACCCTTA	<i>ZnT5-P10R</i> GAGACCAGCCTGACCAACAT	189
<i>ZnT5-P11F</i> CCATCTGGACCCATCAGTCT	<i>ZnT5-P11R</i> CCTGGCCCTGAATTCTTTCT	530
<i>ZnT5-C1F</i> CTGATGACGTGGCTTGGC	<i>ZnT5-C1R</i> CGAAAAGTCCCACAGCCTTC	120
<i>ZnT6-P1F</i> AAGGTGTCAGCAGAGATGG	<i>ZnT6-P1R</i> GGGACTGTCATGATGGGATT	1170
<i>ZnT6-P2F</i> CACCTTCTCACCGTGCCTT	<i>ZnT6-P2R</i> AGGCAGGAGAATTGCTTGAA	1037
<i>ZnT6-P3F</i> TCTCACCCAGGATTCATCTC	<i>ZnT6-P3R</i> TGTAGCACGTGTGTGTTGTCAGA	1168
<i>ZnT5-P4F</i> TTAAGCATTTGGGATGAAGGA	<i>ZnT5-P4R</i> GTGCTCGAGTTTCCCAGAA	1076
<i>ZnT5-P5F</i> GGAGGCCAAGGCAGGTAG	<i>ZnT5-P5R</i> GAATTGCTTGAACCCAGGAG	985
<i>ZnT5-P6F</i> TTTCTTCCTGGCTTGCAGAT	<i>ZnT5-P6R</i> GGTTTCACCATGTTGTGCAG	756
<i>ZnT5-P7F</i> TGGGCAGCTTAAATAACAGAAA	<i>ZnT5-P7R</i> GTGATTCAGCCTTTGGGAAG	468
<i>ZnT5-P8F</i> TCAGCAACCCTAATCCAACC	<i>ZnT5-P8R</i> TGTAGCACGTGTGTTGTCA	496
<i>ZnT5-P9F</i> CGAAAACCTCCTCGTTGCTG	<i>ZnT5-P9R</i> ACTCCAATGACCCCTCCTCT	278

Table 1 continued

Forward primer	Reverse primer	PCR product length (bp)
<i>ZnT5-P10F</i> GGAGGCCAAGGCAGGTAG	<i>ZnT5-P10R</i> ATGGCAAACCCCGTCTC	543
<i>ZnT5-P11F</i> ACCCATCAGAAGAAATAAACCA	<i>ZnT5-P11R</i> ATTTGAGGCCAGGCACAGT	272
<i>ZnT6-C1F</i> TTGACTCCTTGGCTTCCAAT	<i>ZnT6-C1R</i> AAAGGAGAGAACTTTAACAAAAATC	103
<i>ZnT2IE-1F</i> CGTCCTCACTCAGCAACACC	<i>ZnT2IE-1R</i> TCTTCGTTCCCTCACCTCAC	98
<i>ZnT2IE-2F</i> AGGACTCCCATTCCCCTATC	<i>ZnT2IE-2R</i> AGGAGAATAACGTCACCCATGT	128
<i>ZnT2IE-3F</i> ATATTGGTGGCCATTTCAC	<i>ZnT2IE-3R</i> ACAGAGGCCATGGTTGACAT	136
<i>ZnT2IE-4F</i> ATATGAGGGGTGGGGTAAGG	<i>ZnT2IE-4R</i> ACAGCTCCCAGTGTTCTTGG	189
<i>ZnT2IE-5F</i> GCCCTATCTCTCATGGCTGT	<i>ZnT2IE-5R</i> CCACCTACCCTCAGGTTGT	97
<i>ZnT2IE-6F</i> TTCTGAAGTGTGGTCTGTCCTT	<i>ZnT2IE-6R</i> GAAGTCCACACCTGAAGC	84
<i>ZnT2IE-7F</i> TCAGTGTTAAGAGTGGAGAGGAA	<i>ZnT2IE-7R</i> AACCCAGCCTCAGTTTCTT	95
<i>ZnT2IE-8F</i> TACCTGGCAGAGGAATGGAA	<i>ZnT2IE-8R</i> GAAAGGGAACATTTGGCTCA	178
<i>ZnT2IE-9F</i> TATGAATCTGAGCCCCTCCA	<i>ZnT2IE-9R</i> CAAGTGACCAAACCCACCTC	153

Primer names contain the name of the gene, and following abbreviations: *Real* real-time PCR primer, *A-F* primers for coding region sequencing, *P* promoter region primers, *IE* intron–exon primers

Primers to *ZnT4* were designed to GenBank sequence Accession No AF025409

Primers to *ZnT1* were designed to GenBank sequence Accession No AF323590

Primers to *ZnT2* were designed to GenBank sequence Accession No NM_032513

Primers to *ZnT3* were designed to GenBank sequence Accession No U76010

Primers to *ZnT5* were designed to GenBank sequence Accession No AF461760

Primers to *ZnT6* were designed to GenBank sequence Accession No XM_059432

Primers to *ZnT7* were designed to GenBank sequence Accession No AY094606

Primers to *ZnT8* were designed to GenBank sequence Accession No AY117411

Primers to *ZnT9* were designed to GenBank sequence Accession No BC016949

Primers to *ZnT10* were designed to GenBank sequence Accession No AY117411

Primers to β -actin were designed to GenBank sequence Accession No E00829

gel, and the right size bands were excised, purified and sent for sequencing to Monash Sequencing Centre, Melbourne. Results were aligned to the original sequence using Sequencer software to identify any modifications.

Transcription binding motif analysis

Transcription binding motifs relevant to lactation and metal homeostasis were identified manually by scanning the binding motif sequences through the promoter region for the two different transporters SLC30A5 and SLC30A6.

Western blots

Western blots were performed as previously described (Michalczyk et al. 2003). Briefly, cell pellets were resuspended in 10 ml of lysis buffer and disrupted by passing through a 25-gauge needle 8–10 times followed by sonication on ice with a Microson Ultrasonic cell disruptor (Misonix Incorporated, NY, USA). Samples were then stored at -80°C until needed for analysis. Quantification of protein concentrations in cell lysates was performed using BSA protein assay kit (ThermoLab

System), following the manufacturer's instructions. Protein samples were prepared with 6× loading dye, and a Page Ruler™ Prestained Protein ladder (Fermentas) was used as a protein molecular weight marker. Sixty micrograms of each extract was fractionated by SDS-PAGE using Bio-Rad Mini Protein Gel system according to manufacturer's instructions. Proteins were transferred to nitrocellulose membranes (Pal Gelman) using a Trans-Blot Transfer Cell (Bio-Rad). Blots were incubated overnight at 4 °C with monoclonal antibodies for SLC30A5 (Kambe et al. 2002), diluted at 1:500 and SLC30A6 (Abnova mouse monoclonal #H00055676-M01) diluted at 1:250 in 1 % casein. Proteins were detected using 1:4000 dilution of horseradish peroxidase-conjugated sheep anti-mouse antibody and chemiluminescence detection kit (Roche Diagnostic) according to manufacturer's instructions. Images were captured using the Luminescent Image Analyser LAS-3000 (Fujifilm). Membranes were re-probed with β-actin antibody (diluted 1 in 2000) and processed as above. β-Actin and Ponceau S stains were used as controls. Densitometry, using Fuji Film Multi Gauge V3.0 computer software, was performed to quantify results, and ratios for protein levels were calculated relative to β-actin and Ponceau S stains.

Immunofluorescence

Fibroblasts from patients and controls and PMC42-LA cells were grown on 10-mm-diameter glass cover slips. BT blocks (1 cm³) were immersed in OCT (Tissue Tek; Sydney, Australia) and frozen in liquid nitrogen for 3 min followed by sectioning (8–10 μm thickness) on gelatin (5 %)-coated slides using Leica CM1800 cryostat at between –17 and –20 °C. At around 50 % confluency, coverslips with cells were rinsed with PBS (after 48 h for M17 treated chambers) and fixed in 4 % paraformaldehyde (Sigma-Aldrich; Sydney, Australia) for 5, 10 min for BT. After two washes with PBS, they were permeabilized with 0.1 % TX-100 (Sigma-Aldrich; Sydney, Australia) for 10 min (BT 5 % for 5 min) followed by blocking in 1 % BSA for 10 min (BT 3 % for 90 min). Cells were incubated overnight at 4 °C with primary antibody diluted in 1 % BSA in PBS (SLC30A5 1/100, SLC30A6 1/75). After PBS washes, a secondary antibody Alexa Fluor 488 anti-mouse (Chemicon, Melbourne, Australia) diluted at 1:2000 was added and samples were incubated for 2 h at room temperature following by PBS washes. Coverslips were mounted on glass slides using ProLong Gold antifade reagent (Invitrogen; Melbourne, Australia). Confocal images were obtained using a Leica confocal microscope system TCS SP2 (Leica; Melbourne, Australia).

SLC30A5 and SLC30A6 pyrosequencing assay

Bisulphite pyrosequencing for DNA methylation analysis

Bisulphite conversion of DNA was performed using EZ DNA Methylation Gold™ kit (Zymo Research) following the manufacturers' protocol. Briefly, 2 μg of genomic DNA was incubated with CT conversion reagent and incubated at the following temperatures; 98 °C for 10 min, 64 °C for 2.5 h and held at 4 °C. DNA was then transferred to a spin column, washed, de-sulfonated, purified and finally eluted in a 10 μl volume.

Quantitative bisulphite pyrosequencing was used to determine the percentage methylation at individual CpG sites within the SLC30A5 and SLC30A6 promoter regions (NT_022184.15; 11212499-11212863). Briefly, 0.2 μg of bisulphite-treated DNA was added as a template in PCR using 12.5 μl Hot Star Taq mastermix (Qiagen), total volume 25 μl. Primer sequences and PCR conditions are given in Table 1. Biotin-labelled PCR products were captured with streptavidin Sepharose beads (GE Healthcare) and made single-stranded using a Pyrosequencing Vacuum Prep Tool (Qiagen). Sequencing primers were annealed to the single-stranded PCR product by heating to 80 °C, followed by slow cooling. Pyrosequencing was then carried out on a Pyromark MD system. Cytosine methylation was quantified using proprietary PyroQ CpG 1.0.6 software. All PCR and pyrosequencing reaction were carried out in duplicate.

Assay validations were carried out to rule out any amplification bias of primers for methylated DNA and to assess assay reproducibility using methods described previously (White et al. 2006). All primers were found to be unbiased and data reproducible. Zero and 100 % methylated controls (Epitect control DNA, Qiagen, 59568) were routinely run alongside samples as internal controls.

Transcription factor binding site analysis

Transcription factor binding motifs relevant to lactation and metal homeostasis were identified manually by scanning the promoter regions of the *hZnT5* and *hZnT6* genes for the binding motif sequences. To identify transcription factor binding motifs in the proximity of differentially methylated regions, genomic sequences were entered into MatInspector (Genomatix Software—<http://www.genomatix.de/en/index.html>).

Statistical analysis

Data distributions were examined by the Kolmogorov–Smirnov test, and all data sets were normally distributed. Analysis of variance was used to examine methylation in

patients versus controls and type of sample (lymphocytes versus fibroblasts), and the interaction between these fixed factors, at each individual CpG, and across the mean of the investigated CpGs in a given gene. A p value of <0.05 was considered statistically significant.

Results

Alkaline phosphatase activity was reduced in patient (Mother 1 and Mother 2) lymphoblasts

Significantly reduced alkaline phosphatase activity was found in patient lymphoblast (Mother 1 and Mother 2) relative to control, pooled lymphoblasts (Fig. 2). In fibroblasts, alkaline phosphatase levels were low, and no significant differences were detected between Mother 1, Mother 2 and pooled controls. Alkaline phosphatase activity was also detected in PMC42-LA cells and healthy BT.

mRNA expression levels of zinc transporters *SLC30A5* and *SLC30A6* were reduced in patient cells

Expression levels of mRNA for all ten zinc exporters were measured in control, Mother 1 and Mother 2 cells using real-time PCR to detect changes in gene expression at transcription level. The control reactions lacking either primers and or template cDNA were negative for all analysed samples. The dissociation curve analysis of all PCR products revealed the single peaks of expected T_m (data not shown), confirming the specificity of all designed primers. The transcript levels of both *SLC30A5* and *SLC30A6* were significantly lower in lymphoblasts from Mother 1 (*SLC30A5* 0.26 ± 0.12 ;

SLC30A6 0.22 ± 0.12) compared to healthy controls (*SLC30A5* 1 ± 0.11 and *SLC30A6* 1 ± 0.09) ($p < 0.05$, t test; Fig. 3a). In Mother 2, transcript levels of *SLC30A5* were significantly lower in lymphoblasts (*SLC30A5* 0.35 ± 0.08) compared to controls (*SLC30A5* 1 ± 0.22), but there was no significant decrease in *SLC30A6* (0.81 ± 0.1) compared to controls (1 ± 0.15) ($p < 0.05$, t test) (Fig. 3a). In fibroblasts from Mother 2, *SLC30A5* and *SLC30A6* transcript levels (*SLC30A5* 0.14 ± 0.09 ; *SLC30A6* 0.4 ± 0.11) were lower than in the control (*SLC30A5* 1 ± 0.12 and *SLC30A6* 1 ± 0.13 ; Fig. 3b).

No differences in the mRNA expression levels of *SLC30A1*, *SLC30A3*, *SLC30A4*, *SLC30A7*, *SLC30A9* and *SLC30A10* of fibroblasts and lymphoblasts from Mother 1 and Mother 2 were found relative to corresponding control lymphoblast and fibroblast levels ($p > 0.05$, t test; Fig. 3a, b). Neither *SLC30A2* nor *SLC30A8* mRNA transcripts were found in either fibroblasts or lymphoblasts from patients or controls. As the mammary gland was the source of the zinc-deficient milk, human BT was analysed for the presence of *SLC30A5* and *SLC30A6* transcripts. *SLC30A6* transcripts were 48 times more abundant than *SLC30A5* transcripts in normal mammary tissue (Fig. 3c).

Sequence analysis of *SLC30A2* from patients cells showed no gene mutations

As *SLC30A2* has previously been linked with zinc-deficient patient's disorder, the open reading frame (ORF) of *SLC30A2* was sequenced from lymphoblasts and fibroblasts of patients and corresponding controls. No nucleotide differences were seen between control, Mother 1 and Mother 2. Exon–intron splice variants were also analysed

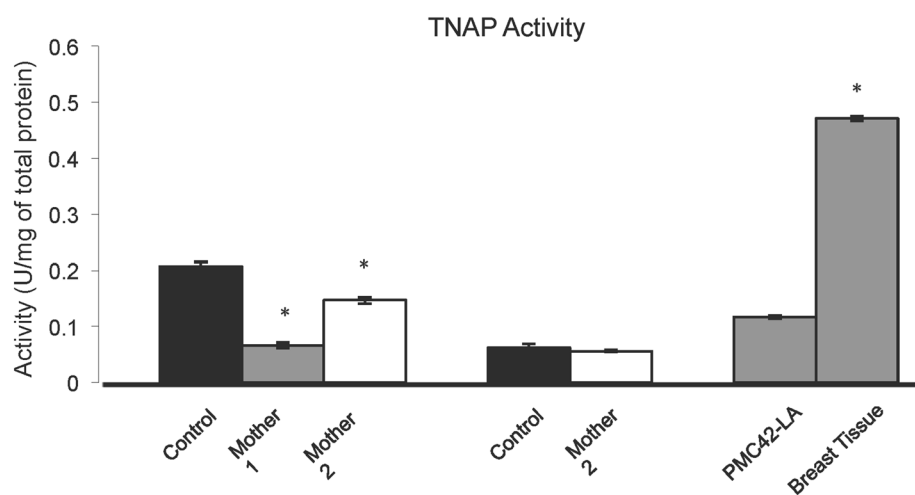


Fig. 2 Tissue non-specific alkaline phosphatase activity (TNAP). Total TNAP activity was detected at 405 nm wavelength, using p-nitrophenol as a substrate, in lymphoblasts, fibroblasts, PMC-42 mammary epithelial cells and breast tissue from both patients and

control. Significant decreases were found in ALP activity in Mother 1 and Mother 2 lymphoblasts compared to control lymphoblasts. No differences were found between Mother 2 and control fibroblasts. Values represent mean of triplicates \pm SEM, * $p \leq 0.05$

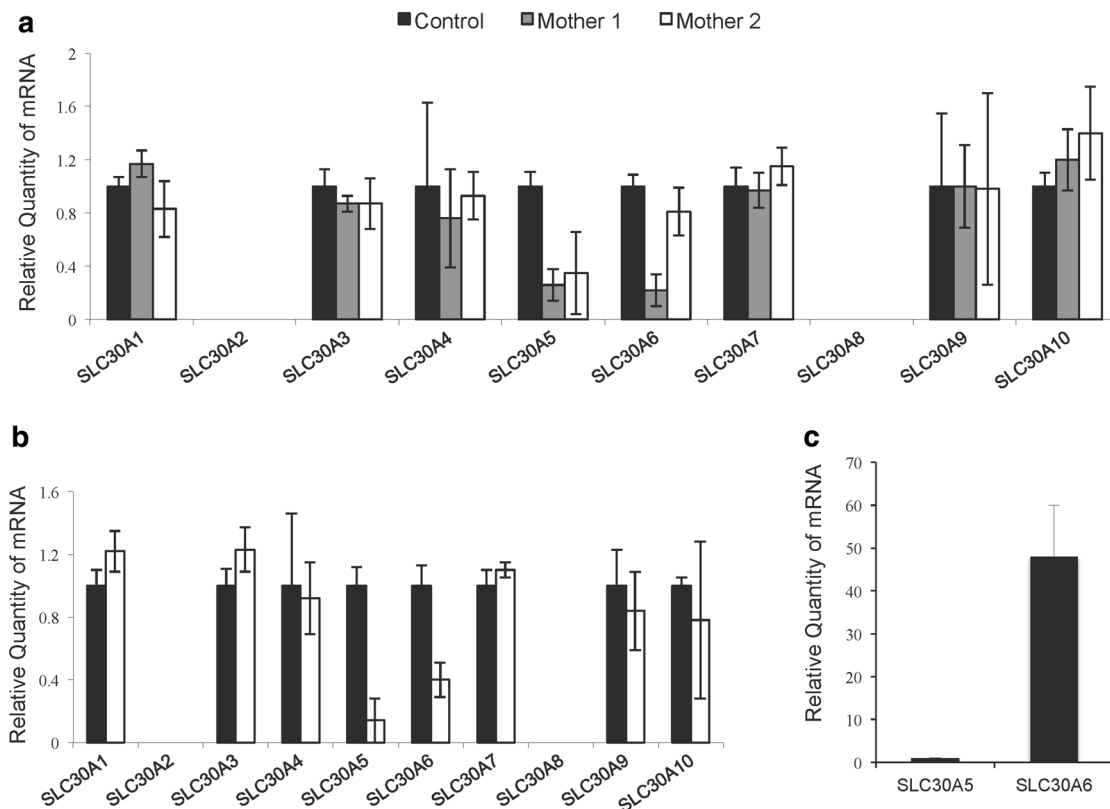


Fig. 3 Real-time RT-PCR analysis of SLC30A mRNAs isolated from cells of Mother 1, Mother 2 and corresponding controls. **a** Comparison of *SLC30A1*, *SLC30A2*, *SLC30A3*, *SLC30A4*, *SLC30A5*, *SLC30A6*, *SLC30A7*, *SLC30A8*, *SLC30A9* and *SLC30A10* relative mRNA expression levels between lymphoblasts of Mother 1 and corresponding controls. A significant reduction in *SLC30A5* and *SLC30A6* transcript levels was detected in Mother 1 lymphoblasts compared to controls ($p < 0.05$, t test). No differences were observed in relative mRNA expression levels of *SLC30A1*, *SLC30A3*, *SLC30A7*, *SLC30A9* and *SLC30A10* in lymphoblasts from Mother 1 and Mother 2 versus controls ($p > 0.05$, t test). There was no detectable expression of

SLC30A2 or *SLC30A8* in lymphoblasts. **b** Comparison of *SLC30A1*, *SLC30A2*, *SLC30A3*, *SLC30A4*, *SLC30A5*, *SLC30A6*, *SLC30A7*, *SLC30A8*, *SLC30A9* and *SLC30A10* relative mRNA expression levels between fibroblasts of Mother 1 and corresponding control. A significant reduction in *SLC30A5* and *SLC30A6* mRNA in Mother 1 fibroblasts was found compared to controls ($p < 0.05$, t test). There was no detectable expression of *SLC30A2* or *SLC30A8* in fibroblasts. **c** In human resting breast tissue, *SLC30A5* and *SLC30A6* expressions were detected and a 48-fold difference was observed between *SLC30A5* and *SLC30A6* transcript levels. Values represent mean of triplicates \pm SEM, $*p \leq 0.05$

using nine different sets of primers (Table 1) corresponding to alternative splice sites for the *SLC30A2* gene. No changes were observed for this transporter.

Sequence analysis of SLC30A5 and SLC30A6 cDNA showed no differences between patient and control cells

As there was reduced expression of *SLC30A5* and *SLC30A6* mRNA in fibroblast and lymphoblast cells from Mother 1 and Mother 2 compared to corresponding control cells, sequence analysis of cDNA was carried out to detect changes in the coding regions of these genes. In *SLC30A5* (GenBank AF461760), two single nucleotide modifications at positions 1692 (C \rightarrow T) and 1800 (T \rightarrow A) from start codon were identified in some control and patient cells.

These modifications did not alter the amino acid sequence of *SLC30A5*.

cDNA sequencing indicated no differences in the coding region of the *SLC30A6* gene between patients and corresponding controls and in all lymphoblasts tested (both patients and controls). A full-length *SLC30A6* message and a variant that was missing 43 nucleotides starting from position 216 (Fig. 4a) were found in lymphoblasts. Similarly, in all fibroblasts (patients and controls) two versions of *SLC30A6* ORF were detected, one full length and another with 49 nucleotides missing from position 757 to 806 from start codon (Fig. 4b). Sequence analysis was also performed at 5' and 3' untranslated regions (UTR) of *SLC30A5* and *SLC30A6* genes to find any changes present in the micro-RNA binding regions, but no differences were found between patient and control samples.

Analysis of exon–intron structure of the *SLC30A6* gene showed no differences between patient and control cells

To investigate whether the different *SLC30A6* mRNA variants found in fibroblast and lymphoblast cells were due to alternate splicing, analysis of exon–intron structure of the gene was performed. The genomic sequence of *SLC30A6* was obtained using BLASTn search of human genome available from GenBank. The *SLC30A6* gene consists of 14 exons positioned on chromosomes 2p22.3. In lymphoblasts from both control and patients, two splice site variants were identified, a full-length message and a variant missing exon 4 (42 nucleotides). In the fibroblasts, a deletion of 48 nucleotides produced a truncated version of *SLC30A6* mRNA (lacking exon 9), which coexisted with full-length message in these cells (Fig. 4c).

Promoter analysis showed no differences between patient and control cells

To establish whether reduced levels of *SLC30A5* or *SLC30A6* were due to changes in the promoter regions of these genes, sequence analysis was carried out on the DNA up to 4000 base pairs upstream from the start codons of *SLC30A5* and *SLC30A6* (Fig. 5). This region contained the following transcriptional regulatory elements: metal responsive element (MRE), STAT-5 (binding site for prolactin), TATA binding site, progesterone responsive element (PRE), gonadotrophin-responsive element (GRE) and insulin-responsive element (IRE). Point changes were observed at position –1155 (T→:), –1325 (G → C) from the start codon and –545 (A → G), –1735 (C → T) in control and Mother 1 fibroblasts for *SLC30A5* and *SLC30A6*, respectively, but did not affect the above-mentioned important transcription binding sites.

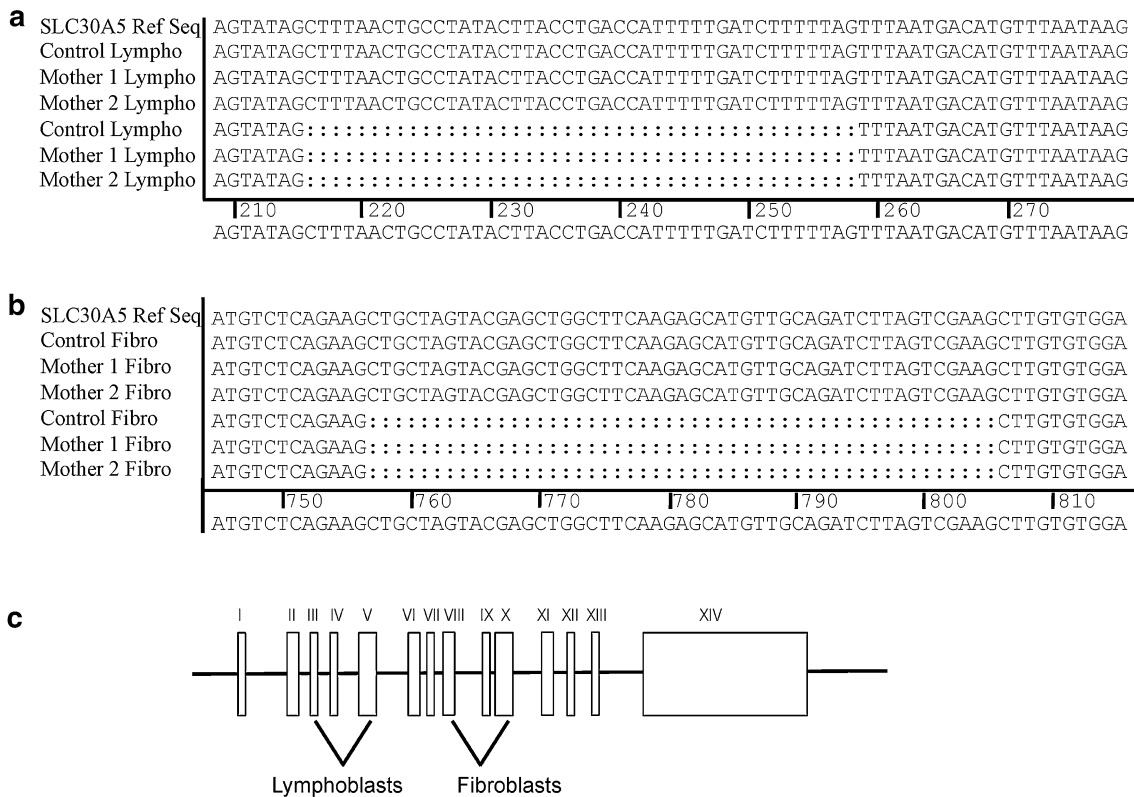


Fig. 4 Analysis of fragments of *SLC30A6* cDNA from lymphoblasts and fibroblasts from Mother 1, Mother 2 and corresponding controls to elucidate splice site variants. **a, b** Fragment of *SLC30A6* cDNA from lymphoblast and fibroblast showing a deletion of 43 and 49 nucleotides (double dots), respectively, in control, Mother 1 and Mother 2, along with full-length cDNA. **c** Diagram illustrating the

different exon–intron structure of the *SLC30A6* gene. In lymphoblasts, the full-length mRNA coexisted with the alternatively spliced form (missing exon IV); in fibroblasts, an alternatively spliced form of *SLC30A6* which did not show exon IX was present, together with the full-length version of mRNA

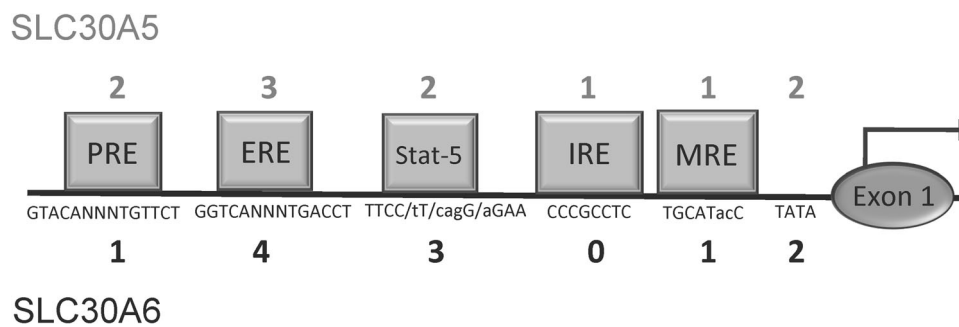


Fig. 5 Diagrammatic representation of significant transcription binding factors present 4000-bp upstream of the translation start point. The location and order of the indicated transcription binding factors shown here are only approximate as *SLC30A5* and *SLC30A6* have multiple binding sites for different transcription factors. For both these genes, the number of binding sites present in the sequence is

indicated by a number adjacent to the gene names. Abbreviations used in the diagram: PRE (progesterone-responsive element), ERE (oestrogen-responsive element), Stat-5 (binding site for prolactin), IRE (insulin-responsive element) and MRE (metal-responsive element)

Western blot analysis of SLC30A5 and SLC30A6 proteins showed reduced levels in patient cells

Western blot analysis was used to detect both SLC30A5 and SLC30A6 proteins in patient and control fibroblasts and lymphoblasts. A significant reduction in SLC30A5 and SLC30A6 proteins was observed for Mother 1 and Mother 2 lymphoblasts compared to control lymphoblasts (Fig. 6a, b). No changes were observed in fibroblasts for SLC30A6 protein expression. There was a significant reduction in SLC30A5 of Mother 2 fibroblasts. In lymphoblasts, the major band detected with the SLC30A5 antibody was 57 kDa, and a less intense band was seen at 55 kDa. For fibroblasts, a single band of 55 kDa was detected (Fig. 6a). In lymphoblasts, no differences in SLC30A5 band sizes were seen between control and Mother 1 and Mother 2. Using the SLC30A6 antibody, two bands (55 and 57 kDa) with equal intensity were found in lymphoblasts and one band of 55 kDa in fibroblasts (Fig. 6b). Lysates of the human breast carcinoma line PMC42-LA and human BT were tested for the presence of SLC30A5 and SLC30A6 proteins. The SLC30A5 antibody detected a weak band of size 57 kDa in PMC42-LA cell extracts while a strong band of 55 kDa was seen in BT (Fig. 6a). The SLC30A6 antibody showed negligible amounts of SLC30A6 in the PMC42-LA cells and a strong band at 55 kDa in the BT (Fig. 6b).

Intracellular localization of SLC30A5 and SLC30A6 was similar in patient and control cells

Confocal microscopy of fibroblasts from Mother 2 and control showed both SLC30A5 and SLC30A6 proteins to be localized in small vesicles throughout the cytoplasm (Fig. 7a, b, e, f). Lymphoblasts also showed a similar distribution of SLC30A5 and SLC30A6 across the

cytoplasm for patients and control (data not shown). A similar localization pattern for both zinc exporters was observed for PMC42 cells (Fig. 7c, g). Sections of normal BT showed these transporters to be localized to specific regions of the tissue (Fig. 7d, h).

DNA methylation patterns in lymphoblast were different between patients and control cells

SLC30A5 methylation

In lymphoblasts, CpG site 2 was found to be significantly less methylated in Mother 1 (4 %) and Mother 2 (4 %) compared with control samples (13 %; Fig. 8a). In contrast, the reverse was seen in fibroblasts where Mother 2 methylation (52 %) was greater than in the control sample (38 %; Fig. 8b). Methylation levels at all four sites were significantly higher in fibroblasts than lymphoblasts with the exception of CpG 1 and CpG 2 for the controls (Fig. 8a, b).

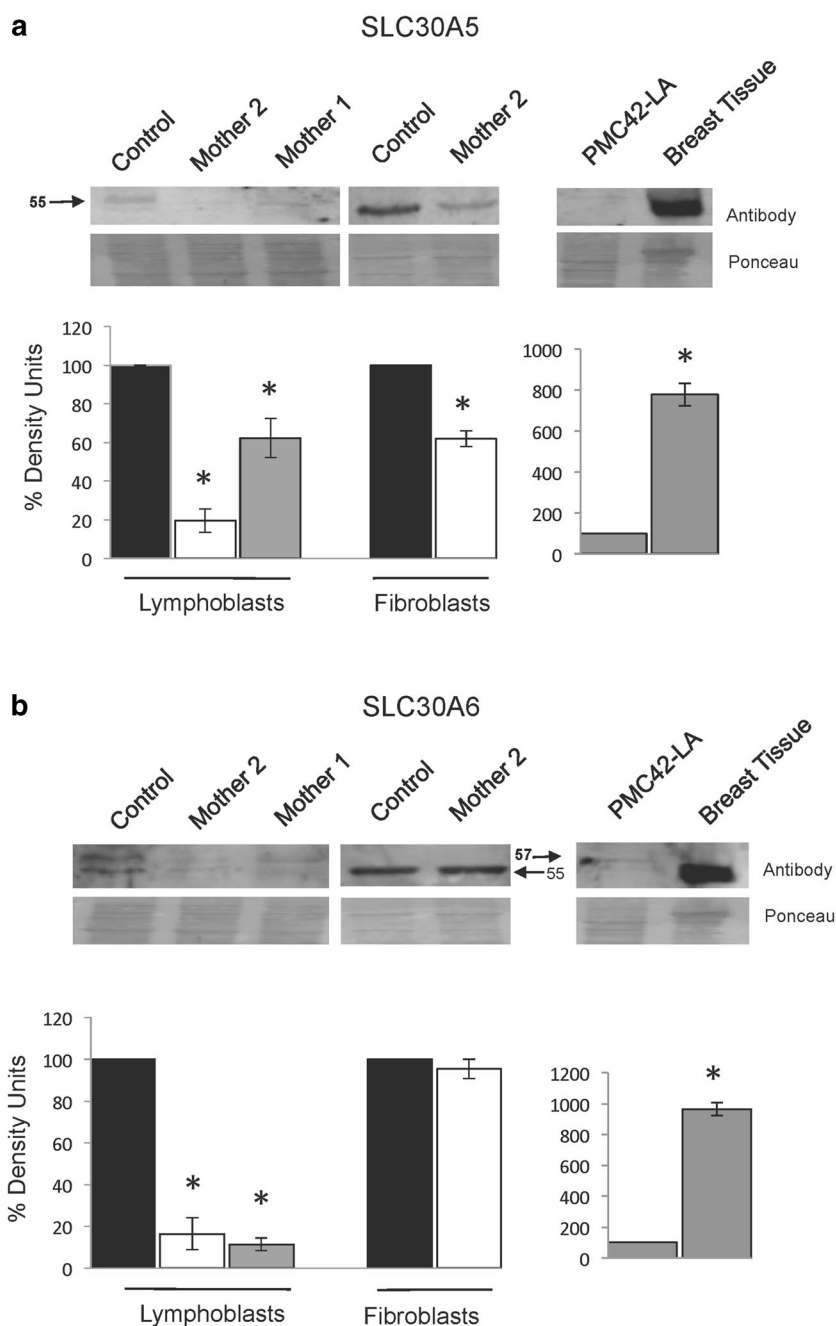
SLC30A6 methylation

Methylation within the SLC30A6 gene was below the detectable levels in lymphoblast and fibroblast extracts from Mother 1, Mother 2 and control.

Discussion

In two affected women, low levels of zinc in the maternal milk combined with a response by the infants to zinc therapy indicated a defect in the maternal breast affecting secretion of zinc into milk. The observation that neither mother was suffering from zinc deficiency suggested that specific defects to zinc exporters in the mothers' BT were involved in this pathology.

Fig. 6 Western blot analysis of proteins from two mothers with zinc-deficient infants. Expression levels of SLC30A5 and SLC30A6 protein were analysed in cells from Mother 1 and Mother 2. **a** For SLC30A5, bands of the predicted size of 57 kDa were detected in all lymphoblasts, and bands of 55 kDa were present in all fibroblasts, for both Mother 1, Mother 2 and controls. A band of 57 kDa was detected in PMC42 cells, and a band of 55 kDa was found in normal breast tissue (BT). **b** For SLC30A6, two bands of approximately 55 and 57 kDa were detected in lymphoblasts from Mother 1, Mother 2 and control cells, while in fibroblasts a 55 kDa band was found in Mother 2 and controls. A band between 55 and 57 kDa was detected in PMC42 cells and normal breast tissue. An antibody to housekeeping human β -actin, along with Ponceau S, was used to indicate the relative levels of protein, and densitometry was performed to quantify the results. Values represent mean of triplicates \pm SEM, * $p \leq 0.05$



We found significant reductions in the TNAP activity of lymphoblasts from Mother 1 and Mother 2 relative to control lymphoblasts, consistent with zinc/zinc transporter activity required for the activity of TNAP (Suzuki et al. 2005). In fibroblasts, TNAP activity was very low, consistent with other studies, which may have accounted for the lack of differences detected between the affected mothers and the control. The reduced TNAP in lymphoblasts is consistent with a reduced function of zinc export in the Mother 1 and Mother 2 cells relative to controls.

Missense mutations in *SLC30A2* (ZnT2) have been reported to underlie cases of maternal defects of zinc secretion into milk, based on analysis of DNA extracted from mother's blood cells (Chowanadisai et al. 2006; Itsumura et al. 2013; Lasry et al. 2012). In contrast to this, we found no detectable *SLC30A2* mRNA in either lymphoblasts or fibroblasts from the two mothers who produced zinc-deficient milk. Sequence analysis of the ORF and exon-intron splice variants performed on patient and control samples from the two different cell types showed no changes, confirming that ZnT2 mutations were not responsible for this

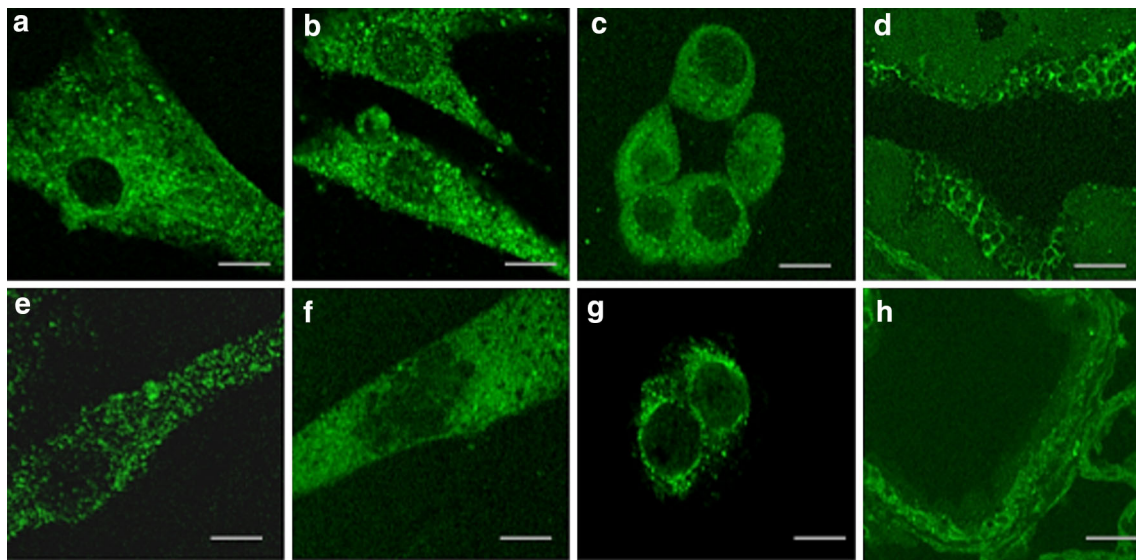


Fig. 7 Immunocytochemical localization of SLC30A5 and SLC30A6. Immunostaining to detect SLC30A5 (a–d) and SLC30A6 (e–h) was carried out on control fibroblasts (a, e) Mother 2 fibroblasts (b, f) PMC-42 (c, g) and cryosections of human breast tissue (d, h). Fibroblasts grown on coverslips and lymphoblasts grown in suspension were fixed with 4 % paraformaldehyde and stained with

SLC30A5 and SLC30A6 antibodies, respectively, followed by secondary antibody conjugated with Alexa 488. SLC30A5 and SLC30A6. Images show vesicular cytoplasmic and perinuclear localization of SLC30A5 (a, b, c, d) and SLC30A6 (e, f, g, h) in control fibroblast, Mother 2 fibroblasts, PMC-42LA and human breast tissue, respectively. Bar 20 μ m

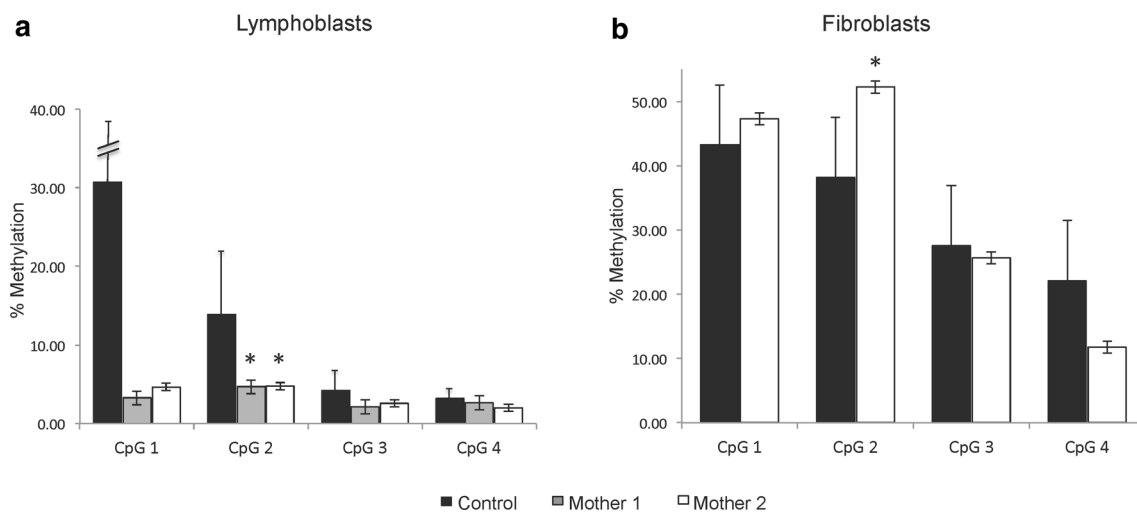


Fig. 8 Bisulphite pyrosequencing for DNA methylation of SLC30A5 and SLC30A6 genes. Quantitative bisulphite pyrosequencing was used to determine the percentage methylation at individual CpG sites within the *SLC30A5* and *SLC30A6* promoter regions. **a** For SLC30A5,

lymphoblasts CpG site 2 was significantly less methylated in Mother 1 (4 %) and Mother 2 (4 %) compared with control samples (13 %). **b** In fibroblasts, Mother 1 methylation (52 %) was greater than in the control sample (38 %)

disorder. This raised the possibility that another molecular defect could be responsible for this condition. More than one member of the solute carrier family SLC30 may participate in the export of zinc into milk or there may be some redundancy amongst zinc transporters. This possibility is supported by observations that in mothers with mutations SLC30A2, some zinc was still present in the milk (Itsumura et al. 2013; Lasry et al. 2012).

Analysis of transcription of all 10 members of the mammalian *SLC30A* family showed that reduced levels of *SLC30A5* mRNA were observed from fibroblasts and lymphoblasts of Mother 1 and Mother 2 compared to controls. A reduction in *SLC30A6* transcripts was found in lymphoblasts and fibroblasts from Mother 1 but not in Mother 2, relative to control cells. Thus, defects in *SLC30A5* and/or possibly *SLC30A6* may underlie this

disorder. We verified that both mRNA and proteins of these transporters were present in mammary tissue obtained from breast biopsies. Both *SLC30A5* and *SLC30A6* are located in the early secretory pathway (Huang and Gitschier 1997; Kambe 2011; Kambe et al. 2002; Kirschke and Huang 2003); thus, the *SLC30A5* transporter may have a compatible role in sequestration of zinc into vesicles destined for secretion from mammary epithelial cells.

Cells from Mother 1, Mother 2 and controls contained alternative splice variants of *SLC30A6*. In lymphoblasts, in addition to the full-length transcript, a variant that lacked exon IV was present. In fibroblasts, a variant that lacked exon IX was detected in addition to the full-length transcript. Similar transcripts were found in extracts from both mothers and controls, indicating that the alternate splicing was not associated with the zinc-deficient phenotype. Splice variants of *SLC30A5* differing have previously been found in Caco-2 cells, where one form contained all 17 exons, while the other lacked exons 1, 2, 4 and exons 15–17, (Jackson et al. 2007; Thornton et al. 2011). We did not detect splice variants of *SLC30A5* in either lymphoblasts or fibroblasts.

Protein analysis indicated the presence of two isoforms for each of *SLC30A5* and *SLC30A6*, corresponding to bands of 55 and 57 kDa in lymphoblasts. A 55 kDa band was the only band seen in fibroblasts, possibly due to the low abundance of the protein or alternatively our antibody only detected the full-length protein. A 55 kDa protein was also the single dominant band in the normal BT. The band sizes detected in both mothers and control were consistent with previously reported sizes of 55 and 57 and 60 kDa found in a range of human cells and tissues (Cragg 2008; Cragg et al. 2002; Kambe et al. 2002). Identified bands of 55 kDa for the *SLC30A6* protein corresponded with predicted size of the splice variant found in lymphoblasts where exon IV was missing 42 nucleotides (Fig. 4).

The protein levels of *SLC30A5* and *SLC30A6* in lymphoblasts and fibroblasts were measured to establish if they were reduced, consistent with the mRNA data. In lymphoblasts from affected mothers, both *SLC30A5* and *SLC30A6* protein levels were reduced compared to the control. In fibroblasts however, the protein levels of *SLC30A6* of cells from the affected mothers were no different from the control, for reasons that are not clear.

Both *SLC30A6* mRNA and protein were more strongly expressed in normal BT than in isolated lymphoblasts and fibroblasts. The high expression of the transporters in normal breast cannot necessarily be attributed to a greater expression in mammary epithelial cells as the BT also contains many cell types including adipocytes, endothelial cells and smooth muscle cells. The mammary gland *SLC30A6* mRNA levels were 48 times more expressed than *SLC30A5*. Assuming that *SLC30A5/SLC30A6* also

operates as a heterodimer in BT, then *SLC30A6* may have additional functions in the mammary gland.

SLC30A5 and *SLC30A6* form heterodimers, and this oligomerization is required for their zinc transport function (Kambe 2012). *SLC30A6* is not directly involved in zinc transport across the cell membrane as it does not have a zinc-binding site within the trans-membrane domain, but it may function as a modulator (Fukunaka et al. 2009). Thus, if one of either *SLC30A5* or *SLC30A6* protein is reduced, it may impair the function of the dimer in transporting zinc.

Both *SLC30A5* and *SLC30A6* possess a number of hormone-responsive elements including MRE, STAT-5, TATA binding site, PRE, GRE and IRE that strongly support a function for these transporters in mammary function in particular milk secretion which is controlled by prolactin. To detect changes in these binding sites of the promoter region of *SLC30A5* and *SLC30A6*, promoter analysis was performed on sequences up to 4000-bp upstream of the translation start site. No changes were observed within these binding sites. miRNA analysis of the 3' region of these also revealed no changes.

Since CpG islands are present in the promoter region of the *SLC30A5* and *SLC30A6* genes, their expression may be regulated by promoter methylation. DNA methylation is involved in the down-regulation of members of the SLC family of transporters (Gonen et al. 2008; Hong et al. 2005; Kikuchi et al. 2006; Philibert et al. 2007; Zschocke et al. 2007). We investigated whether DNA methylation was associated with the altered levels of *SLC30A5* and *SLC30A6* transcripts found in cells from mothers producing zinc-deficient milk. In lymphoblasts, the methylation percentage of CpG site 1 in *SLC30A5* was 6–7 times lower in Mothers 1 and 2 compared to the controls. However, due to the large variation in methylation within the control samples, the differences between Mothers 1 and 2 and controls were not significant. In the same cells, the methylation of *SLC30A5* measured at CpG site 2 was 65 % lower in both Mother 1 and Mother 2 relative to control lymphoblasts. In fibroblasts, conversely, the percentage methylation at CpG site 2 was greater by 20 % in Mother 2 relative to the controls, and at CpG site 4 the methylation was 45 % lower in Mothers 2 compared to the controls.

Hypermethylation at the CpG site 2 in fibroblasts could be responsible for the lower level of expression of the *SLC30A5* gene. In lymphoblasts, this CpG site was hypomethylated in affected mothers compared with controls, but expression levels were reduced at both the mRNA and protein levels. Although promoter DNA hypermethylation rather than hypomethylation is generally regarded as the suppressive epigenetic modification, this relationship is not always found and methylation may be suppress or enhance gene expression depending on cell type (Ions et al. 2013). The difference in DNA methylation at CpG site 2

between affected mothers and controls could thus contribute to the differences in gene expression observed in both lymphoblasts and fibroblasts.

We detected no DNA methylation in the promoter region of *SLC30A6* and thus can only conclude that differences in gene expression were not associated with DNA methylation in this region. We cannot exclude the possibility that DNA methylation in other regions of the *SLC30A6* gene differed between the affected mothers and controls.

In summary, we report two cases of zinc deficiency in neonates caused by a defect in the transport of zinc into milk. Both cases are associated with significant reduction in both *SLC30A5* and *SLC30A6* mRNA and protein from cells from the mothers producing the zinc-deficient milk. Defects in these two transporters have not previously been implicated in neonatal zinc deficiency. Promoter analysis showing changes in methylation state to CpG site 2 in lymphoblasts, while not definitive, suggests that the expression of *SLC30A5* may be modified by methylation and could potentially account for the reduced activity of *SLC30A5* and low level of zinc in milk.

References

- Ackland ML, Mercer JF (1992) The murine mutation, lethal milk, results in production of zinc-deficient milk. *J Nutr* 122:1214–1218
- Aggett PJ, Atherton DJ, More J, Davey J, Delves HT, Harries JT (1980) Symptomatic zinc deficiency in a breast-fed preterm infant. *Arch Dis Child* 55:547–550
- Bye AM, Goodfellow A, Atherton DJ (1985) Transient zinc deficiency in a full-term breast-fed infant of normal birth weight. *Pediatr Dermatol* 2:308–311
- Chowanadisai W, Lönnnerdal B, Kelleher SL (2006) Identification of a mutation in *SLC30A2* (ZnT-2) in women with low milk zinc concentration that results in transient neonatal zinc deficiency. *J Biol Chem* 281:39699–39707. doi:10.1074/jbc.M605821200
- Connors TJ, Czarnecki DB, Haskett MI (1983) Acquired zinc deficiency in a breast-fed premature infant. *Arch Dermatol* 119:319–321
- Cragg MS (2008) The potential effect of statins on rituximab immunotherapy. *PLoS Med* 5:e77. doi:10.1371/journal.pmed.0050077
- Cragg RA et al (2002) A novel zinc-regulated human zinc transporter, hZTL1, is localized to the enterocyte apical membrane. *J Biol Chem* 277:22789–22797. doi:10.1074/jbc.M200577200
- Fukunaka A et al (2009) Demonstration and characterization of the heterodimerization of ZnT5 and ZnT6 in the early secretory pathway. *J Biol Chem* 284:30798–30806. doi:10.1074/jbc.M109.026435
- Glover MT, Atherton DJ (1988) Transient zinc deficiency in two full-term breast-fed siblings associated with low maternal breast milk zinc concentration. *Pediatr Dermatol* 5:10–13
- Gonen N, Bram EE, Assaraf YG (2008) GCFT/SLC46A1 promoter methylation and restoration of gene expression in human leukemia cells. *Biochem Biophys Res Commun* 376:787–792. doi:10.1016/j.bbrc.2008.09.074
- Heinen F, Matern D, Pringsheim W, Leititis JU, Brandis M (1995) Zinc deficiency in an exclusively breast-fed preterm infant. *Eur J Pediatr* 154:71–75
- Hong C et al (2005) Shared epigenetic mechanisms in human and mouse gliomas inactivate expression of the growth suppressor *SLC5A8*. *Cancer Res* 65:3617–3623. doi:10.1158/0008-5472.CAN-05-0048
- Huang LK, Gitschier J (1997) A novel gene involved in zinc transport is deficient in the lethal milk mouse. *Nat Genet* 17:292–297
- Ions LJ et al (2013) Effects of Sirt1 on DNA methylation and expression of genes affected by dietary restriction. *Age* 35:1835–1849. doi:10.1007/s11357-012-9485-8
- Itsumura N, Inamo Y, Okazaki F, Teranishi F, Narita H, Kambe T, Kodama H (2013) Compound heterozygous mutations in *SLC30A2/ZnT2* results in low milk zinc concentrations: a novel mechanism for zinc deficiency in a breast-fed infant. *PLoS ONE* 8:e64045. doi:10.1371/journal.pone.0064045
- Jackson KA, Helston RM, McKay JA, O'Neill ED, Mathers JC, Ford D (2007) Splice variants of the human zinc transporter ZnT5 (*SLC30A5*) are differentially localized and regulated by zinc through transcription and mRNA stability. *J Biol Chem* 282:10423–10431. doi:10.1074/jbc.M610535200
- Kambe T (2011) An overview of a wide range of functions of ZnT and Zip zinc transporters in the secretory pathway. *Biosci Biotechnol Biochem* 75:1036–1043
- Kambe T (2012) Molecular architecture and function of ZnT transporters. *Curr Top Membr* 69:199–220. doi:10.1016/B978-0-12-394390-3.00008-2
- Kambe T et al (2002) Cloning and characterization of a novel mammalian zinc transporter, zinc transporter 5, abundantly expressed in pancreatic beta cells. *J Biol Chem* 277:19049–19055. doi:10.1074/jbc.M200910200
- Khoshoo V, Kjarsgaard J, Krafchick B, Zlotkin SH (1992) Zinc deficiency in a full-term breast-fed infant: unusual presentation. *Pediatrics* 89:1094–1095
- Kikuchi R, Kusuhara H, Hattori N, Shiota K, Kim I, Gonzalez FJ, Sugiyama Y (2006) Regulation of the expression of human organic anion transporter 3 by hepatocyte nuclear factor 1alpha/beta and DNA methylation. *Mol Pharmacol* 70:887–896. doi:10.1124/mol.106.025494
- Kirschke CP, Huang L (2003) ZnT7, a novel mammalian zinc transporter, accumulates zinc in the Golgi apparatus. *J Biol Chem* 278:4096–4102. doi:10.1074/jbc.M207644200
- Lasry I et al (2012) A dominant negative heterozygous G87R mutation in the zinc transporter, ZnT-2 (*SLC30A2*), results in transient neonatal zinc deficiency. *J Biol Chem* 287:29348–29361. doi:10.1074/jbc.M112.368159
- Lee DY, Shay NF, Cousins RJ (1992) Altered zinc metabolism occurs in murine lethal milk syndrome. *J Nutr* 122:2233–2238
- Michalczyk A, Varigos G, Catto Smith A, Blomeley R, Ackland L (2003) Analysis of zinc transporter, hZnT4 (*Slc30A4*) gene expression in a mammary gland disorder leading to reduced zinc secretion into milk. *Hum Genet* 113:202–210
- Parker PH, Helinek GL, Meneely RL, Stroop S, Ghishan FK, Greene HL (1982) Zinc deficiency in a premature infant fed exclusively human milk. *Am J Dis Child* 136:77–78
- Philibert R, Madan A, Andersen A, Cadoret R, Packer H, Sandhu H (2007) Serotonin transporter mRNA levels are associated with the methylation of an upstream CpG island. *Am J Med Genet B Neuropsychiatr Genet* 144B:101–105. doi:10.1002/ajmg.b.30414
- Piletz JE, Ganschow RE (1978) Zinc deficiency in murine milk underlies expression of the lethal milk (lm) mutation. *Science* 199:181–183

- Prasad AS (1985) Clinical manifestations of zinc deficiency. *Annu Rev Nutr* 5:341–363
- Sharma NL, Sharma RC, Gupta KR, Sharma RP (1988) Self-limiting acrodermatitis enteropathica. A follow-up study of three inter-related families. *Int J Dermatol* 27:485–486
- Stevens J, Lubitz L (1998) Symptomatic zinc deficiency in breast-fed term and premature infants. *J Paediatr Child Health* 34:97–100
- Suzuki T, Ishihara K, Migaki H, Ishihara K, Nagao M, Yamaguchi-Iwai Y, Kambe T (2005) Two different zinc transport complexes of cation diffusion facilitator proteins localized in the secretory pathway operate to activate alkaline phosphatases in vertebrate cells. *J Biol Chem* 280:30956–30962. doi:[10.1074/jbc.M506902200](https://doi.org/10.1074/jbc.M506902200)
- Thornton JK, Taylor KM, Ford D, Valentine RA (2011) Differential subcellular localization of the splice variants of the zinc transporter ZnT5 is dictated by the different C-terminal regions. *PLoS ONE* 6:e23878. doi:[10.1371/journal.pone.0023878](https://doi.org/10.1371/journal.pone.0023878)
- Weymouth RD, Kelly R, Lansdell BJ (1982) Symptomatic zinc deficiency in a premature infant. *Aust Paediatr J* 18:208–210
- White HE, Durston VJ, Harvey JF, Cross NC (2006) Quantitative analysis of SNRPN (correction of SRPN) gene methylation by pyrosequencing as a diagnostic test for Prader–Willi syndrome and Angelman syndrome. *Clin Chem* 52:1005–1013. doi:[10.1373/clinchem.2005.065086](https://doi.org/10.1373/clinchem.2005.065086)
- Whitehead RH, Monaghan P, Webber LM, Bertoncello I, Vitali AA (1983) A new human breast carcinoma cell line (PMC42) with stem cell characteristics. II. Characterization of cells growing as organoids. *J Nat Cancer Inst* 71:1193–1203
- Zimmerman AW, Hambidge KM, Lepow ML, Greenberg RD, Stover ML, Casey CE (1982) Acrodermatitis in breast-fed premature infants: evidence for a defect of mammary zinc secretion. *Pediatrics* 69:176–183
- Zschocke J, Allritz C, Engele J, Rein T (2007) DNA methylation dependent silencing of the human glutamate transporter EAAT2 gene in glial cells. *Glia* 55:663–674. doi:[10.1002/glia.20497](https://doi.org/10.1002/glia.20497)